construction materials

MDPI

Article

Studies on Optimization of Fly Ash, GGBS and Precipitated Silica in Geopolymer Concrete

Anilkumar [1], K S Sreekeshava [2,*] and C Bhargavi [2]

[1] Department of Civil Engineering, Government Engineering College, Raichur, Affiliated to Visvesvaraya Technological University, Belagavi 590018, India; anilkumarsahukar@gmail.com
[2] Department of Civil Engineering, Jyothy Institute of Technology, Affiliated to Visvesvaraya Technological University, Belagavi 590018, India; bhargavi.c@jyothyit.ac.in
* Correspondence: sreekeshava.ks@jyothyit.ac.in

Abstract: Considering the urgent need for sustainable construction materials, this study investigates the mechanical and microstructural responses of novel hybrid geopolymer concrete blends incorporating Fly Ash (FA), Ground Granulated Blast Furnace Slag (GGBS), Cement (C) and Precipitated Silica (PS) as partial replacements for traditional cementitious materials. The motive lies in reducing CO_2 emissions associated with Ordinary Portland Cement (OPC). The main aim of the study was to optimise the proportions of industrial wastes for enhanced performance and sustainability. The geopolymer mixes were activated using a 10 M sodium hydroxide (NaOH)—Sodium Silicate (Na_2SiO_3) solution and cast into cubes (100 mm), cylinders (100 mm × 200 mm) and prism specimens for compressive, split tensile and flexural strength testing, respectively. Six combinations of mixes were studied: FA/C (50:50), GGBS/C (50:50), FA/C/PS (50:40:10), FA/GGBS/PS (50:40:10), GGBS/C (50:50) and GGBS/FA/PS (50:40:10). The results indicated that the blend with 50% FA, 40% GGBS and 10% PS exhibited higher strength. Mixes with GGBS and PS presented a l0 lower slump due to rapid setting and higher water demand, while GGBS-FA-cement mixes indicated better workability. GGBS/C exhibited a 24.6% rise in compressive strength for 7 days, whereas FA/C presented a 31.3% rise at 90 days. GGBS/FA mix indicated a 35.5% strength drop from 28 days to 90 days. SEM and EDS analyses showed that FA-rich mixes had porous microstructures, while GGBS-based mixes formed denser matrices with increased calcium content.

Keywords: geopolymer concrete; GGBS; fly-ash; precipitated silica; SEM; EDS

check for updates

Received: 11 March 2025
Revised: 16 April 2025
Accepted: 18 April 2025
Published: 24 April 2025

Citation: Anilkumar; Sreekeshava, K.S.; Bhargavi, C. Studies on Optimization of Fly Ash, GGBS and Precipitated Silica in Geopolymer Concrete. *Constr. Mater.* **2025**, *5*, 29. https://doi.org/10.3390/constrmater5020029

Copyright: © 2025 by the authors. Licensee MDPI, Basel, Switzerland. This article is an open access article distributed under the terms and conditions of the Creative Commons Attribution (CC BY) license (https://creativecommons.org/licenses/by/4.0/).

1. Introduction

Concrete is the most widely used construction material in the world, second only to water in terms of overall consumption. The production of Portland cement, being the primary ingredient of concrete, significantly contributes to the pollution of the environment, with the cement industry accounting for 5% of global CO_2 emissions [1]. This is mainly due to the combustion of fossil fuels in rotary kilns and the chemical breakdown of limestone. Further, quarrying of the raw materials leads to depletion of natural resources, requiring up to 1.6 tons of raw materials for every ton of cement that is being produced [1]. Despite the concerns, concrete is an essential entity due to its ease of preparation and versatility.

To mitigate such environmental impacts, geopolymer concrete offers a sustainable alternative by reducing the dependency on Portland cement, thus conserving the resources and also addressing the problem of industrial waste disposal. Geopolymer Concrete (GC) is found to be an eco-friendly alternative to the conventional Portland cement-based concrete.

This is because, unlike the traditional concrete, which depends on Portland Cement as a binder, GC forms through the process of geopolymerisation. This process resembles the natural clay formation in which alkaline activators (AA) break and rearrange the Silica (SiO_2) and Alumina (Al_2O_3) in to 3-dimensional polymeric structure. Here, the traditionally used cement is replaced with a geopolymer binder when alumino-silicate materials react with AA such as Sodium Hydroxide (NaOH) or Sodium Silicate (Na_2SiO_3). A strong binding material is generated that holds the aggregates together without the hydration process. Unlike the hydration process in the Portland cement-based concrete, GC undergoes chemical transformation.

Longo et al. highlighted the potential of lightweight geopolymer mortars for retrofitting buildings, while Tayeh et al. studied the effects of elevated temperatures on the durability of GPC [2,3]. Waste and recycled materials exhibited an opportunity in reducing the carbon footprint of cement-based systems. Incorporation of waste glass powder by Celik et al. and recycled PET aggregates by Coviello et al. in matrices improved the sustainability without compromising the performance [4–6]. Studies by Coviello et al. also presented that hybrid mixtures that combined waste materials with additives which are carbon-based can result in enhanced mechanical and thermal behaviour of concrete [7].

Fly-ash-based geopolymer concrete was initially studied by Davidovits et al., in which a basic foundation was laid for geopolymer concrete [8]. The study demonstrated that fly-ash-based geopolymer concrete achieved comparable strength along with reduced environmental impact. Research by Silva et al. introduced the role of alkali activators in enhancing the polymeric chain for improved strength [9]. Manjunath et al. illustrated the blending of fly ash with GGBS to enhance the early strength due to increased content of calcium, thus accelerating geopolymerisation [10]. Studies performed by Hemalatha et al. revealed that adding precipitated silica improved the microstructure through refinement of pore sizes, in turn contributing to enhanced strength [11]. The strength characteristics of geopolymer concrete were extensively studied by Hardjito et al. The results presented that optimisation of alkaline concentrations and curing conditions are significant factors influencing the development of the strength [12]. A study by Rajamane et al. highlighted that the geopolymer concrete exhibited a specific tensile behaviour and correlated compressive strength with tensile behaviour [13]. Zhang et al. highlighted that geopolymer concrete microstructure plays a crucial role in indicating denser matrices formed by fly ash and GGBS combinations [14]. Albitar et al. indicated that GGBS-based geopolymer concrete offered improved resistance to sulphate attack and better performance during aggressive environments [15]. Van Deventer et al. demonstrated that geopolymer concrete significantly reduced carbon footprint by reducing cement consumption [16]. A study by Reddy et al. confirmed that silica fume additions improved bonding by reducing microcracking [17]. Research by Subramaniam et al. highlighted that higher NaOH molarity enhanced the polymerisation process, positively impacting the strength performance [18]. A study by Singh et al. indicated that the calcium-rich GGBS-based geopolymer concrete results in faster setting times and improved strength development [19]. Zhao et al. presented that geopolymer concrete exhibited lower shrinkage rates than traditional concrete [20]. Kumar et al. demonstrated that the addition of precipitated silica leads to improved pore structure refinement [21].

While multiple studies explored the geopolymer concrete using individual binders such as FA or GGBS, there are limited research works with respect to hybrid combinations of FA, GGBS, Cement and PS. The synergistic effects of including multiple binders, especially the inclusion of PS, which includes high pozzolanic reactivity and finer particle size, remain unexplored. Existing studies have focused on early-age strength development, overlooking performance in the long-term. Furthermore, there is a lack of clarity on how hybrid binder

combinations influence key microstructural features such as porosity, gel morphology and phase composition. This gap is crucial, as understanding the interaction between these binders can help optimise geopolymer mixes for both improved mechanical performance and durability. Thus, the study aims to fill the gap by systematically evaluating the effects of hybrid binder combinations on strength and microstructure.

2. Materials and Methods

2.1. Material Characterisation

Class F fly ash and GGBS were collected from Raichur Thermal Power Station, Raichur, Karnataka, India. FA met the requirements of ASTM C618 for use in cementitious systems. FA exhibited a loss on ignition (LOI) of 5.44%, a moisture content of 1.8% and a fineness limit of 29%. GGBS, a byproduct of the steel exhibited a Blaine's fineness of 480 m^2/kg, moisture content of 0.9% and bulk density of 1000 kg/m^3. PS, a chemically synthesised form of SiO_2 with a particle size of 80 nm, specific surface area of 176 m^2/g and bulk density of 72 kg/m^3, was sourced from Mithra Increst Private Limited, Bangalore, Karnataka, India. NaOH, available as solid pellets, was used in a molar concentration of 10 M. The NaOH solution was prepared by dissolving the pellets in distilled water and allowed to rest for 24 h in order to cool [22]. Na_2SiO_3 solution had a SiO_2:Na_2O ratio of 2:1. The solutions were mixed in the ratio of 2.5:1 by volume and stirred thoroughly to get a homogeneous mixture [23].

When mixed with fly ash or GGBS, the AA dissolves the aluminosilicate minerals, thus releasing Silicon (Si^{4+}) and Aluminium (Al^{2+}) ions into the solution. These ions further react with hydroxide (OH^-) to form aluminosilicate gel, which acts as the binding phase, similar to the calcium silicate hydrate (C-S-H) structure in traditional concrete. Figure 1 presents the materials considered in this study.



Figure 1. Materials Sourced for the Study.

The normal consistency of the cement sample was determined to be 29% with an initial setting time of 100 min. The specific gravity of cement was found to be 2.87. The fly ash sample exhibited a normal consistency of 32% and an initial setting time of 330 min. The GGBS sample exhibited a normal consistency of 32% and an initial setting time of 45 min. The specific gravity of GGBS was found to be 2.91. The specific gravity of fine aggregates was found to be 2.62 with a maximum bulking of 38.46%. The fineness modulus of fine aggregates was 3.16. The fineness modulus of coarse aggregates was found to be 9.37.

2.2. Sample Characterisation

Six different combinations were considered for this study. Each combination involved different proportions of Fly-ash, GGBS and Precipitated Silica, as indicated in Table 1.

Table 1. Mix Proportions.

Set No.	Sample Combination	Sample Name	Proportions (% Weight of Binder)
1	Fly Ash:Cement	FA/C	50:50
2	GGBS:Fly Ash	GGBS/FA	50:50
3	Fly Ash:Cement:Precipitated Silica	FA/C/PS	50:40:10
4	Fly Ash:GGBS:Precipitated Silica	FA/GGBS/PS	50:40:10
5	GGBS:Cement	GGBS/C	50:50
6	GGBS:Fly Ash:Precipitated Silica	GGBS/FA/PS	50:40:10

The proportions were chosen to reflect a balance between early strength, long-term performance and material synergy. While Fly-ash contributes to sufficient early strength, GGBS contributes to the development of latent hydraulic nature [24]. A balance of the active cementitious materials for early strength later-age properties of raw materials is hence considered in this study. Since Precipitated Silica has a surface area of 200 m^2/g, which reacts rapidly with calcium hydroxide from cement hydration, it is limited to 10% to optimise performance, as excess silica may cause increased water demand.

2.3. Testing Methods

2.3.1. Slump Test

The workability of geopolymer concrete was assessed using a slump test with a standard slump cone of 300 mm height, 200 mm base diameter and 100 mm top diameter satisfying the conditions as per IS 1199:1959 [25]. The cone was filled with 3 layers, each compacted by 25 strokes using tamping rods. The vertical settlement or slump is measured from the original height of the cone to the highest point of settled concrete. Slump test measurement in pictorial form is represented in Figure 2.



Figure 2. Slump Test.

2.3.2. Casting of Cube Specimen for Compressive Strength Test and Split Tensile Strength

150 mm × 150 mm × 150 mm cube moulds were prepared as per IS 516:1959 for compressive strength testing [26]. The prepared mix was poured into the mould in three layers, each compacted by 25 tamping strokes. The top surface was levelled using a trowel. The concrete cubes were stored at 24 °C to 27 °C in a moisture-controlled environment. The specimens were tested for their compressive strength after 7 days, 28 days and 90 days using a Compression Testing Machine (CTM). The load was applied gradually at a rate of

14 N/mm^2 per minute until failure. The compressive strength (f_c) was calculated using the formula indicated in Equation (1),

$$f_c = \frac{P}{A} \quad (1)$$

where P = Maximum load at failure (N) and A = cross-sectional area of the specimen (mm^2). Casting of cubes for the Compressive Strength Test is presented in Figure 3.



Figure 3. Casting of cubes of the mixes.

A total of 9 specimens for each combination were tested, and the average values were tabulated. Split-tensile strength was performed using a cylindrical specimen with dimensions of 150 mm diameter and 300 mm height as per IS 5816:1999 [27]. Post-curing, the specimen was placed on the lower platen of the CTM, and load was applied at a gradual rate of 1.2 N/mm^2 per minute until the specimen splits along its diameter. The split-tensile strength (f_t) was calculated using Equation (2).

$$f_t = \frac{2P}{\pi DL} \quad (2)$$

where D is the diameter of the cylinder (mm) and L is the length of the cylinder (mm). A total of 9 specimens for each combination were tested, and the average values were tabulated. Further, to ensure reliability of the experimental results, means and standard deviations were calculated to evaluate data spread and repeatability, in line with standard analytical practices [28].

2.3.3. Microstructural Analysis

To examine the surface morphology and microstructural features of the mixes, scanning electron microscopy (SEM) analysis was used. For SEM analysis, smaller fragments of fractured specimens were collected, prior to which they were cleaned using ethanol and dried in a hot air oven at 60 °C for 24 h. The dried samples were then sputter-coated with 10 nm of gold using the JEOL JFC-1600, JEOL Ltd., Tokyo, Japan auto fine coater for improved electrical conductivity. Imaging was further carried out using the JEOL JSM-6510LV, JEOL Ltd., Tokyo, Japan.

For phase identification, X-ray Diffraction (XRD) analysis was conducted using a PANalytical X'Pert PRO diffractometer, PANalytical B.V., Almelo, The Netherlands operating at 40 kV and 30 mA. The sample had to be ground into fine powders (<75 µm) using mortar and pestle to ensure homogeneity [29]. Scanning was performed in the 2θ range of 10° to 70° with a step size of 0.02° and a scan speed of 2°/min.

3. Results

3.1. Effect of Optimisation on Slump of Mix

The slump values ranged between 22.5 mm and 25 mm, indicating a low workability. This can be attributed to unique binder composition and lower water content in geopolymer

mix rather than traditional mix [30]. Set 1 and Set 3 recorded 25 mm average slump values, exhibiting that these combinations maintained a moderate cohesion despite the inclusion of precipitated silica in Set 3 [31]. Attributing to GGBS's faster reaction rate and denser gel formation, set 2 and set 6 recorded 23 mm slump values, indicating reduced flowability [32]. Considering the combined effects of GGBS's rapid setting and precipitated silica's high surface area, which in turn increases the water demand, set 4 exhibited the lowest slump of 22.5 mm. Further, set 5 exhibited a 24 mm slump, which showed a balanced workability alongside effective particle packing. The range of slump values is represented in Figure 4.

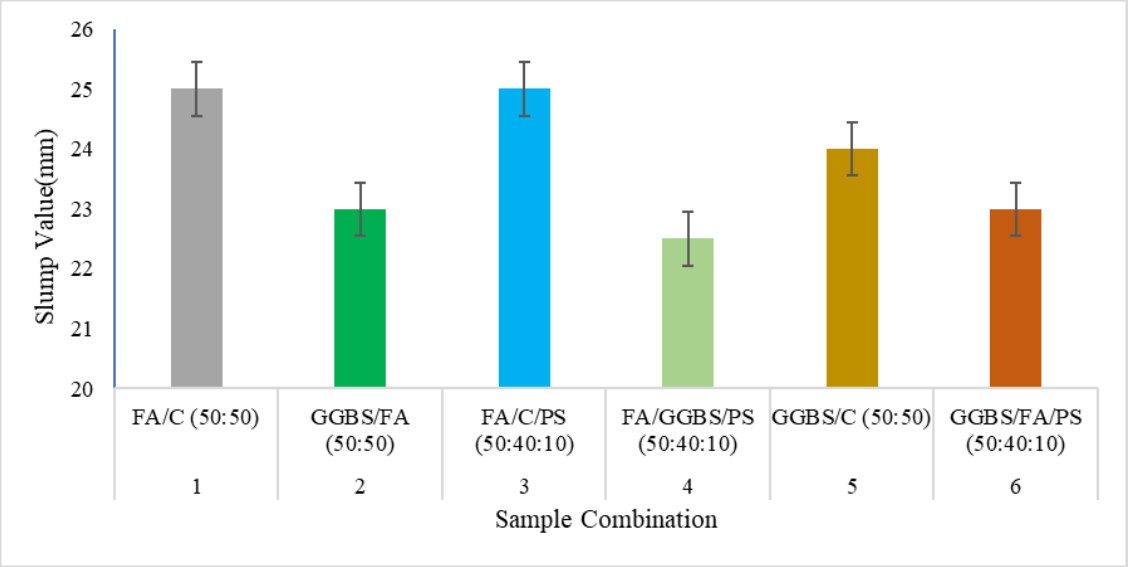

Figure 4. Slump Value Comparison.

3.2. Effect of Optimisation on 7 Days, 28 Days and 90 Days Compressive Strength and Split Tensile Strength

Figure 5 represents the graphical comparison of 7 days, 28 days and 90 days compressive strength. Set 5 exhibited the highest 7-day strength and 28-day strength at 52.31 N/mm^2 and 65.775 N/mm^2, respectively, indicating the fast-reacting nature of GGBS in combination with cement and superior early strength performance [32]. Set 6 closely followed with 52.148 N/mm^2 and 65.33 N/mm^2 indicating that the combination of GGBS and PS contributes to accelerating strength gain due to the refinement of the microstructure [33]. Lowest 7-day strength and 28-day strength were observed at 34.623 N/mm^2 and 47.55 N/mm^2, respectively, indicating a slower pozzolanic reaction, thus requiring prolonged curing for proper strength development [34,35]. The 90-day strength for Set 1 was again found to be highest at 62.755 N/mm^2, demonstrating the long-term strength development potential of fly ash [24]. The positive impact of precipitated silica in sustaining strength was exhibited by set 6 with 58.44 N/mm^2. A substantial drop in strength over time from 59.215 N/mm^2 to 38.22 N/mm^2, mostly due to microcracking or incomplete geopolymerisation, was exhibited by Set 2 [20]. It was hence observed that the GGBS-based mix in set 5 and set 6 exhibits rapid early strength gain, highlighting the GGBS's role in enhancing initial strength. However, set 2 exhibited a notable reduction at 90 days, highlighting the potential shrinkage effects and possible micro-cracking. Fly ash-based mix displayed slower early strength gain but excelled in long-term strength development, reflecting fly-ash's sustained pozzolanic activity. The precipitated silica enhanced mixes showed balanced strength development, which contributed to both early strength improvement attributed to silica's filler effect and long-term stability through micro-structure refinement [11].

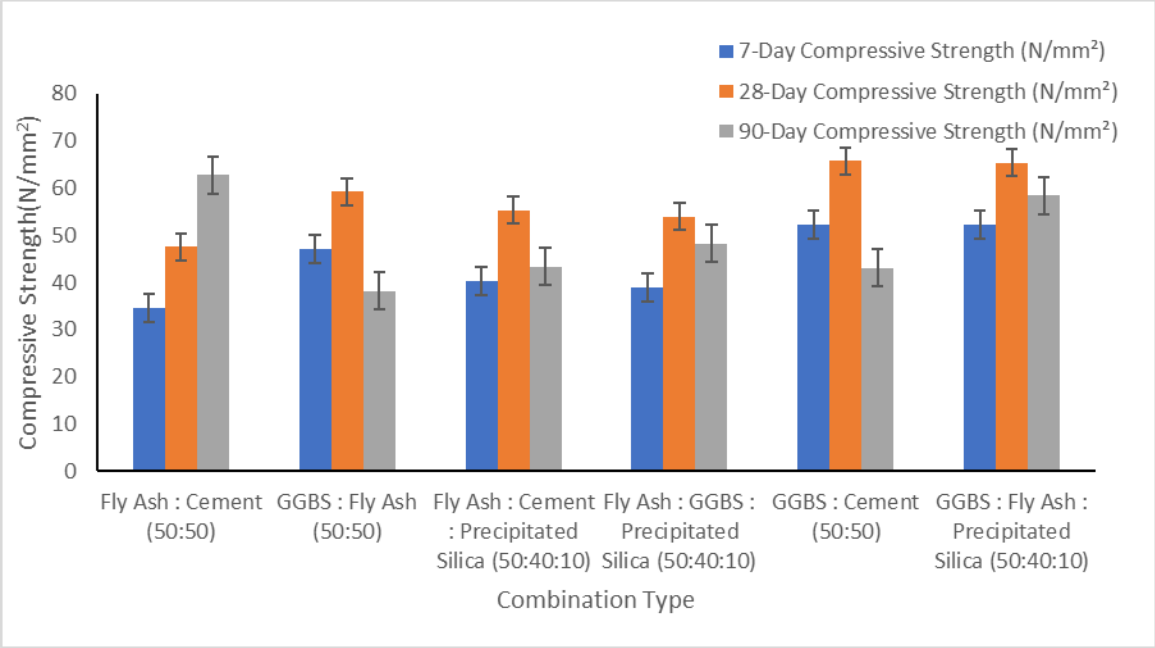

Figure 5. Comparison between 7 days, 28 days and 90 days compressive strength.

Based on the observed damaged patterns in Figure 6, it was observed that Set 1 displayed moderate cracks with relatively lesser surface deterioration, attributing to good bonding with a small degree of brittleness [10]. Since fly-ash and cement mixtures generally develop strength over a period of time through the process of hydration and pozzolanic reactions, only moderate cracking with limited surface damage can be observed, highlighting the fact that fly ash contributes to long-term strength [15]. Set 2 exhibited prominent cracks with material peeling, attributing to incomplete reaction of products, thus weakening the matrix. Set 3 presents distinct, yet controlled, crack patterns highlighting the positive impact of precipitated silica for better packing of particles and pore refinement [17]. The pozzolanic reaction is attenuated due to the presence of silica and the formation of C-S-H gel, thus enhancing the matrix integrity. Set 4 performed well in displaying uniform crack distribution and minimal localised failure, as the combination effectively balances the benefits of GGBS alongside precipitated silica. Set 5, however, suffered extensive surface peeling and delamination attributed to internal shrinkage and poor cohesion [24]. Additionally, GGBS's slower reaction rate as compared to that of cement impacted the early-stage bond, making it weaker. Set 6 exhibited extensive surface damage despite the presence of precipitated silica, attributing to inconsistent activation and weakened bonding. A 35.5% strength reduction was observed in the GGBS/FA/PS mix from 28 to 90 days alongside the similar trends in GGBS-rich mixes. This suggested susceptibility to long-term instability in mixes dominated with GGBS when improperly balanced with other binders. The decline can be attributed to autogenous shrinkage, microcracking and incomplete geopolymerisation resulting from rapid early reaction of GGBS, leaving unreacted bonded phases behind [24].

The split tensile strength results presented in Figure 7 revealed notable variations in strength gain and decline over time. From 7 days to 28 days, Fly-ash-based mixes, set 1, set 3 and set 4 exhibited a 16.95% and 17.85% increase in tensile strength, attributing to Fly Ash's pozzolanic reaction. Conversely, GGBS-dominant mixes (Set-2, Set-5 and Set-6) demonstrated 12.5% lower gains, reflecting GGBS's ability of rapid early strength development. Highlighting the GGBS's rapid hydration capability [35], set 2 and set 5 experienced notable reductions in split tensile strengths of 19.35% and 19.19%, respectively. Set 6 was seen to exhibit stable performance with only a 5.83% decline, highlighting a

well-balanced composition with sustained strength retention. Table 2 summarises the compressive strength and split tensile strength of the mix combinations in the study.



Figure 6. Failure patterns of the mixes under Compression Testing after 90 days.

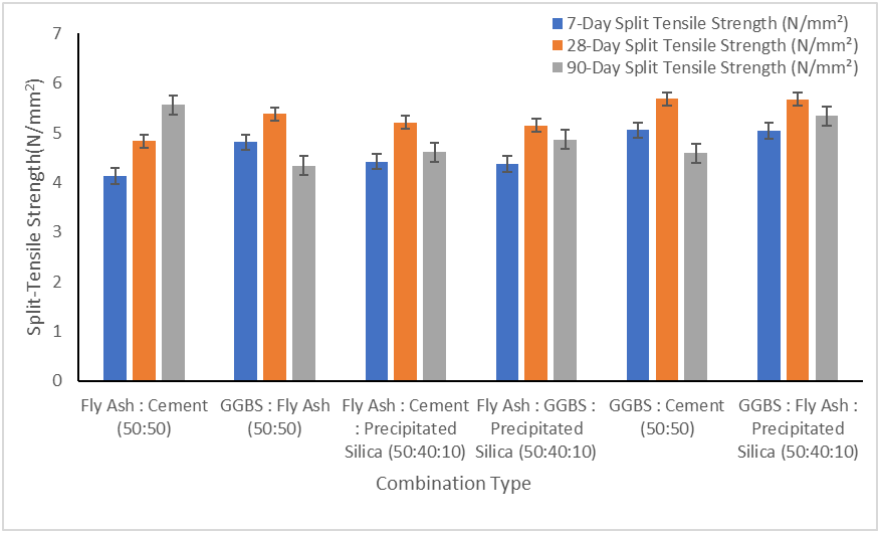

Figure 7. Comparison between 7 days, 28 days and 90 days split-tensile strength.

Table 2. Summary of Strength Results for Different Mix Combinations.

Mix Combination	7-Day Compressive (N/mm^2)	28-Day Compressive (N/mm^2)	90-Day Compressive (N/mm^2)	7-Day Tensile (N/mm^2)	28-Day Tensile (N/mm^2)	90-Day Tensile (N/mm^2)
FA/C	36.55	48.74	62.05	4.55	5.26	5.18
GGBS/FA	52.08	63.65	41.08	5.13	5.78	5.13
FA/C/PS	38.32	50.77	48.52	4.72	5.46	5.14
FA/GGBS/PS	39.01	47.10	44.06	4.67	5.41	5.21
GGBS/C	49.78	67.35	60.11	5.71	6.08	5.62
GGBS/FA/PS	46.55	61.07	55.82	5.63	6.01	5.54

3.3. Effects on Surface Morphology and Internal Structure

As presented in Figure 8, SEM micrographs presented the insights into the surface morphology and the internal structure. SEM images revealed a highly porous microstructure with visible microcracks and loosely bound particles, profoundly due to unreacted fly ash spheres confirming incomplete geopolymerisation of Set 1. The estimated average pore size ranges from 5 to 10 µm contributing to lower packing density. Set 2 exhibited a more compact gel matrix, mainly by C-A-S-H gel, and fewer visible pores as compared to set 1. Fine microcracks of about 1–2 µm width can be evidently observed, mainly due to shrinkage correlating to a 35% reduction in strength from 28 days to 90 days [34]. A moderately dense matrix was observed with mixed phases of C-S-H gel and unreacted particles in Set 3. Incorporation of PS enhanced the fine particles packing, thus improving the 28-day strength. Localised pore clusters of 3 µm suggest higher water demand from PS to reduce long-term strength [32]. A uniform gel phase was observed with minimal microcracking in set 4. Homogeneous gel distribution aligned with a stable trend in mechanical strength from 28 days to 90 days. Porosity is observed to be less than 10%, indicating efficient binder activation. A dense microstructure with well-developed C-S-H and C-A-S-H gel networks was observed in Set 5. Few voids and high particle density explained the peak strength at 28 days [10]. Set 6 was characterised by well-compacted gel regions, strong particle bonding and no major cracks or larger voids. This optimised mix, attributed to consistent strength performance across all testing periods, highlights the combinations of GGBS and PS to enhance the matrix integrity [14].

Figure 9 represents insights into the elemental composition of the concrete mixes utilised for the study. Set 1's spectrum indicated prominent peaks for Si, Al and Ca at relatively lower intensity. Moderate silica and alumina presence and lower calcium content correlate with slow early strength gain with better long-term performance [17]. A notable increase in Ca intensity was visible, thus indicating a higher calcium content presence owing to the presence of GGBS in Set 2. This responds to the aspect of improved early strength development, and the presence of Si and Al attributes to the ongoing geopolymerisation process [36]. The spectrum of Set 3 revealed distinct peaks for Si, Al and moderate Ca content, thus revealing silica-rich phases specifically contributed by precipitated silica. This relates to the balanced mechanical performance observed at 28 days but with reduced long-time strength. Set 4 exhibited a spectrum with intensified Si peaks along with a small presence of Ca. The silica phase, which was combined with calcium-rich compounds, leads to the dense microstructure with stable growth in strength over time. Strong Ca peaks were seen with significant Si and Al levels in the Spectrum of Set 5. This confirms the calcium-rich matrix that supports high early strength gain; however, it aligns with the reduction in 90-day strength due to microcracking [37]. A well-balanced composition of silica-rich

phases with calcium-based hydration products was the reason behind strong peaks for Si, Al and Ca in Set 6's spectrum, which in turn contributes to steady strength development.

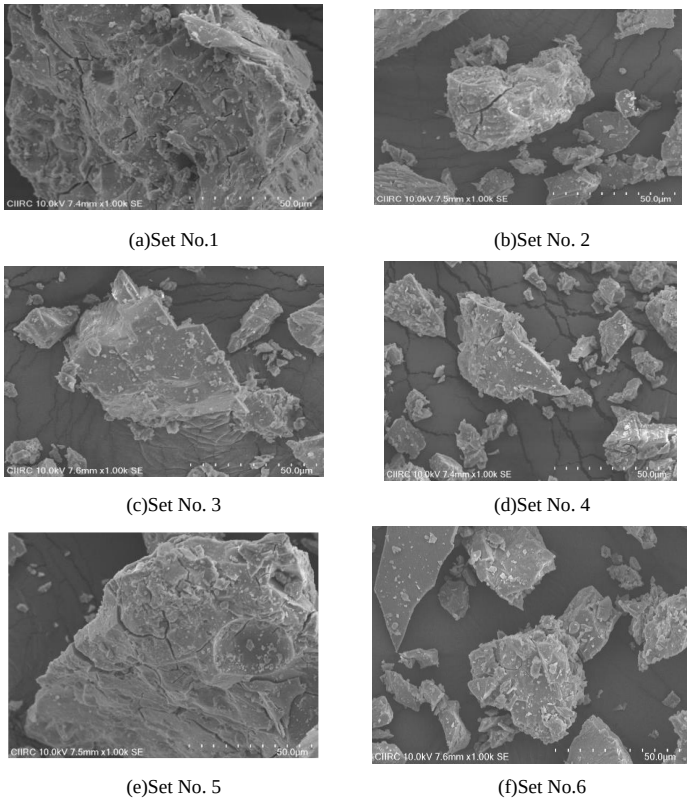

(a)Set No.1 (b)Set No. 2

(c)Set No. 3 (d)Set No. 4

(e)Set No. 5 (f)Set No.6

Figure 8. SEM Analysis of mixes observed at 90 days.

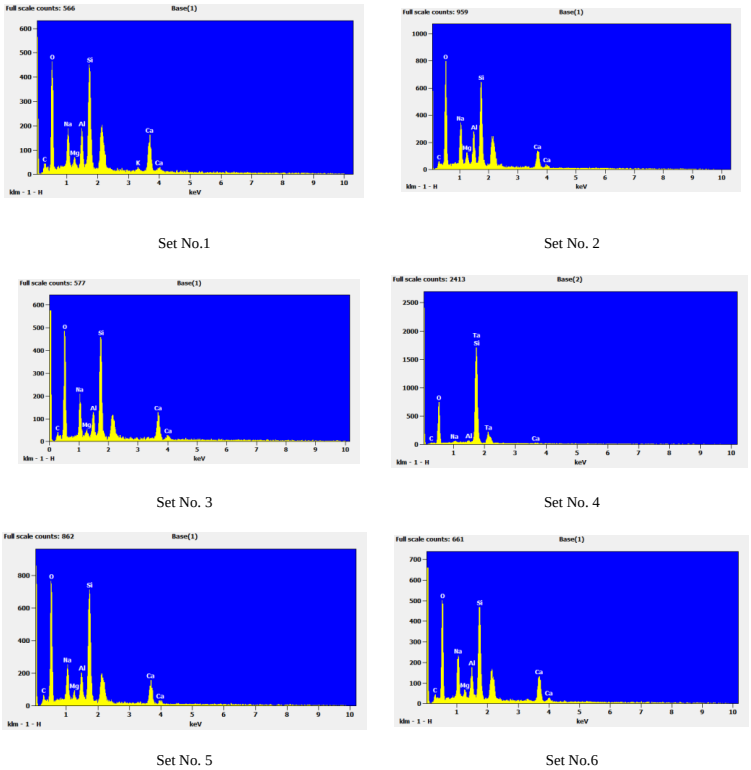

Set No.1 Set No. 2

Set No. 3 Set No. 4

Set No. 5 Set No.6

Figure 9. Energy Dispersive Spectroscopy spectra for the six mixes at 90 days.

4. Conclusions

This study explored the mechanical as well as microstructural properties of hybrid GPC mixes incorporating FA, GGBS, C and PS, which was activated using 10 M alkali solution. The work aimed to understand how each material interacted by varying the binder combinations. The study was performed based on strength development, workability and microstructural evaluation.

The results highlighted that including GGBS and PS significantly enhanced the early setting behaviour and microstructure densification. FA/GGBS/PS (50:40:10) mix presented the lowest slump at 22.5 mm, suggesting limited workability due to the high reactivity of GGBS and the water demand of PS. However, FA/C and FA/C/PS mixes maintained 25 mm slump values, indicating enhanced cohesive properties and better placement characteristics.

With reference to strength development, GGBS/C achieved the highest early compressive strength with a 24.6% increase at 7 days as compared to FA/C. It was observed that FA-based mixes demonstrated superior long-term strength, showing a 31.3% increase in compressive strength at 90 days, suggesting the potential of sustained fly ash performance. The GGBS/FA/PS mix experienced a 35.5% reduction from 28 days to 90 days, attributed to microcracking and incomplete geopolymerisation. FA-incorporated mixtures outperformed other mixes between 7 and 28 days, whereas GGBS-based mixtures exhibited notable decline by 90 days, mainly due to autogenous shrinkage and crack formation. However, the strength profile was observed to be stable for the GGBS/FA/PS mix, highlighting the benefits of interactions between GGBS and PS.

FA/C presented a porous, loosely bound structure indicating slow strength development. However, GGBS/C and GGBS/FA/PS exhibited dense, well-compacted matrices highlighting the enhanced early strength and consistent long-term performance. EDS analysis further revealed that GGBS-based mixes had calcium-rich phases leading to early hydration, while calcium-silica-rich phases were seen in PS-blended mixes, indicating gradual and sustained strength gain.

The findings underscored the usability of hybrid geopolymer binders as sustainable alternatives to conventional cement due to their ability to optimise early strength and long-term performance. Specifically, mixes including both GGBS and PS demonstrated great potential for structural applications, as they require early strength without compromising the durability aspect.

The practical implications from this study include the potential to use the hybrid binders in precast and structural elements where early demoulding is crucial with reduced carbon emissions. However, the sensitivity to curing conditions and water demand variability, particularly with high PS content, is a limitation observed.

The future studies can focus on long-term durability aspects such as carbonation, sulphate resistance and thermal resistance. Alongside that, the water-binder ratio and activator concentration can be optimised for site-based applications.

Author Contributions: Conceptualization, A. and K.S.S.; methodology, A., K.S.S. and C.B.; validation, K.S.S., A. and C.B.; formal analysis, A.; investigation, K.S.S. and A.; resources, A. and C.B.; writing—original draft preparation, A.; writing—review and editing, A., K.S.S. and C.B.; visualization, K.S.S.; supervision, K.S.S. All authors have read and agreed to the published version of the manuscript.

Funding: This research received no external funding.

Data Availability Statement: Data are contained within the article.

Acknowledgments: We thank Jyothy Institute of Technology, Bengaluru, Karnataka, India for facilitating lab equipment support throughout the research process.

Conflicts of Interest: The authors declare no conflicts of interest.

References

1. Coviello, C.G.; La Scala, A.; Sabbà, M.F.; Carnimeo, L. On the Cementitious Mixtures Reinforced with Waste Polyethylene Terephthalate. *Materials* **2024**, *17*, 5351. [CrossRef] [PubMed]
2. Longo, F.; Lassandro, P.; Moshiri, A.; Phatak, T.; Aiello, M.A.; Krakowiak, K.J. Lightweight geopolymer-based mortars for the structural and energy retrofit of buildings. *Energy Build.* **2020**, *225*, 110352. [CrossRef]
3. Tayeh, B.A.; Zeyad, A.M.; Agwa, I.S.; Amin, M. Effect of elevated temperatures on mechanical properties of lightweight geopolymer concrete. *Case Stud. Constr. Mater.* **2021**, *15*, e00673. [CrossRef]
4. Çelik, A.İ.; Tunç, U.; Bahrami, A.; Karalar, M.; Mydin, M.A.O.; Alomayri, T.; Özkılıç, Y.O. Use of waste glass powder toward more sustainable geopolymer concrete. *J. Mater. Res. Technol.* **2023**, *24*, 8533–8546. [CrossRef]
5. Coviello, C.G.; Lassandro, P.; Sabbà, M.F.; Foti, D. Mechanical and thermal effects of using fine recycled PET aggregates in common screeds. *Sustainability* **2023**, *15*, 16692. [CrossRef]
6. Lam, T.-Q.-K.; Vo, T.-T.-T.; Sreekeshava, K.S. Compressive behaviour of reinforced concrete columns using recycled building glass instead of sand aggregate in concrete. *J. Build. Mater. Sci.* **2025**, *7*, 1–19. [CrossRef]
7. Coviello, C.G.; Mansour, S.; Rizzo, F.; Foti, D. An experimental study on the mechanical and thermal properties of graphene-reinforced screeds. In Proceedings of the Fib Symposium, Istanbul, Turkey, 5–7 June 2023; pp. 307–314.
8. Davidovits, J. Geopolymers. *J. Therm. Anal.* **1991**, *37*, 1633–1656. [CrossRef]
9. Silva, P.D.; Sagoe-Crenstil, K.; Sirivivatnanon, V. Kinetics of geopolymerisation: Role of Al_2O_3 and SiO_2. *Cem. Concr. Res.* **2007**, *37*, 512–518. [CrossRef]
10. Manjunath, R.; Ranganath, R.V. Performance Evaluation of Fly-ash based Self-compacting geopolymer concrete mixes. *IOP Conf. Ser. Mater. Sci. Eng.* **2019**, *561*, 012006. [CrossRef]
11. Hemalatha, T.; Gunavadhi, M.; Bhuvaneshwari, B.; Sasmal, S.; Iyer, N.R. Characterization of micro- and nano- modified cementitious system using micro analytical techniques. *Cem. Concr. Compos.* **2015**, *58*, 114–128. [CrossRef]
12. Hardjito, D.; Cheak, C.C.; Lee Ing, C.H. Strength and setting times of low calcium fly ash-based geopolymer mortar. *Mod. Appl. Sci.* **2008**, *2*, 3–11. [CrossRef]
13. Boopalan, C.; Rajamane, N.P. An investigation of bond strength of reinforcing bars in fly ash and GGBS based geopolymer concrete. *MATEC Web Conf.* **2017**, *97*, 01035. [CrossRef]
14. Zhang, Z.; Yao, X.; Zhu, H. Potential application of geopolymers as protection coatings for marine concreteII. Microstructure and anticorrosion mechanism. *Appl. Clay Sci.* **2010**, *49*, 7–12. [CrossRef]
15. Albitar, M.; Mohamed Ali, M.S.; Visintin, P.; Drechsler, M. Durability evaluation of geopolymer and conventional concretes. *Constr. Build. Mater.* **2017**, *136*, 374–385. [CrossRef]
16. Hajimohammadi, A.; van Deventer, J.S.J. Characterisation of One-Part Geopolymer Binders Made from Fly Ash. *Waste Biomass Valorization* **2017**, *8*, 225–233. [CrossRef]
17. Vijaya Bhaskar Reddy, S.; Srinivasa Rao, D.P. Experimental studies on compressive strength of ternary blended concretes at different levels of micro silica and ggbs. *Mater. Today Proc.* **2016**, *3*, 3752–3760. [CrossRef]
18. Bhagath Singh, G.V.P.; Subramaniam, K.V.L. Evaluation of sodium content and sodium hydroxide molarity on compressive strength of alkali activated low-calcium fly ash. *Cem. Concr. Compos.* **2017**, *81*, 122–132. [CrossRef]
19. Malayali, A.B.; Chokkalingam, R.B.; Vinay Singh, M. Experimental study on the compressive strength and permeable properties of GGBS based Geopolymer Pervious Concrete. *IOP Conf. Ser. Mater. Sci. Eng.* **2019**, *561*, 012004. [CrossRef]
20. Zhao, R.; Sanjayan, J.G. Geopolymer and Portland cement concretes in simulated fire. *Mag. Concr. Res.* **2011**, *63*, 163–173. [CrossRef]
21. Kumar, K.S.J.; Seshagiri Rao, M.V.; Reddy, V.S.; Shrihari, S. Performance evaluation of nano-silica concrete. *E3S Web Conf.* **2020**, *184*, 01076. [CrossRef]
22. Srinivasa Reddy, V.; Vamsi Krishna, K.; Seshagiri Rao, M.V.; Shrihari, S. Effect of molarity of sodium hydroxide and molar ratio of alkaline activator solution on the strength development of geopolymer concrete. *E3S Web Conf.* **2021**, *309*, 01058. [CrossRef]
23. Lázaro, A.L.; Rodríguez-Valadez, F.J.; López, J.J.M.; Espejel-Ayala, F. SBA-15 synthesis from sodium silicate prepared with sand and sodium hydroxide. *Mater. Res. Express* **2020**, *7*, 045503. [CrossRef]
24. Xie, J.; Wang, J.; Rao, R.; Wang, C.; Fang, C. Effects of combined usage of GGBS and fly ash on workability and mechanical properties of alkali activated geopolymer concrete with recycled aggregate. *Compos. Part B Eng.* **2019**, *164*, 179–190. [CrossRef]
25. *IS 1199:1959*; Methods of Sampling and Analysis of Concrete. Bureau of Indian Standards: New Delhi, India, 1959.
26. *IS 516:1959*; Methods of Test for Strength of Concrete. Bureau of Indian Standards: New Delhi, India, 1959.
27. *IS 5816:1999*; Splitting Tensile Strength of Concrete—Method of Test. Bureau of Indian Standards: New Delhi, India, 1959.
28. *ASTM E2586-16*; Standard Practice for Calculating and Using Basic Statistics. ASTM International: West Conshohocken, PA, USA, 2016.
29. Moram, M.A.; Vickers, M.E. X-ray diffraction of III-nitrides. Reports on Progress in Physics. *Phys. Soc. (Great Br.)* **2009**, *72*, 036502. [CrossRef]

30. Kumar, S.; Rajendra, S.; Sreekeshava, K.S. Assessment of the shear strength of fly ash-based geopolymer concrete. In *Lecture Notes on Multidisciplinary Industrial Engineering*; Springer: Singapore, 2020; pp. 307–317. [CrossRef]
31. Menadi, B.; Kenai, S. Influence of natural pozzolana content on self-compacting concrete durability properties. *IOP Conf. Ser. Mater. Sci. Eng.* **2018**, *431*, 102011. [CrossRef]
32. Nair, A.; Aditya, S.D.; Adarsh, R.N.; Nandan, M.; Dharek, M.S.; Sreedhara, B.M.; Prashant, S.C.; Sreekeshava, K.S. Additive manufacturing of concrete: Challenges and opportunities. *IOP Conf. Ser. Mater. Sci. Eng.* **2020**, *814*, 012022. [CrossRef]
33. Poornima, N.; Katyal, D.; Revathi, T.; Sivasakthi, M.; Jeyalakshmi, R. Effect of curing on mechanical strength and microstructure of fly ash blend GGBS geopolymer, Portland cement mortar and its behavior at elevated temperature. *Mater. Today Proc.* **2021**, *47*, 863–870. [CrossRef]
34. Bhargavi, C.; Sreekeshava, K.S.; Sunagar, P.; Dharek, M.S.; Ganesh, C.R. Mechanical Properties of Steel and Polypropylene Fiber Reinforced Geopolymer Concrete. *J. Mines Met. Fuels* **2023**, *71*, 984–989. Available online: https://informaticsjournals.co.in/index.php/jmmf/article/view/34783 (accessed on 14 March 2024).
35. Dharek, M.S.; Sunagar, P.; Sreekeshava, K.S.; Nagashree, B.; Thejaswi, P.; Kilabanur, P.; Nruthya, K.; Satish Chandra, C. Experimental investigations on strength performance of the brick produced by blending demolished waste with pozzolanic materials. In *Advances in Sustainable Construction Materials*; Springer: Singapore, 2021; pp. 573–583. [CrossRef]
36. Vyas, S.; Mohammad, S.; Pal, S.; Singh, N. Strength and durability performance of fly ash based geopolymer concrete using nano silica. *Int. J. Eng. Sci. Technol.* **2020**, *4*, 1–12. [CrossRef]
37. Zain, M.F.M.; Karim, M.R.; Islam, M.N.; Hossain, M.M.; Jamil, M.; Al-Mattarn, H.M.A. Prediction of strength and slump of silica fume incorporated high-performance concrete. *Asian J. Sci. Res.* **2015**, *8*, 264–277. [CrossRef]

Disclaimer/Publisher's Note: The statements, opinions and data contained in all publications are solely those of the individual author(s) and contributor(s) and not of MDPI and/or the editor(s). MDPI and/or the editor(s) disclaim responsibility for any injury to people or property resulting from any ideas, methods, instructions or products referred to in the content.